IL NUOVO CIMENTO **39 C** (2016) 352
DOI 10.1393/ncc/i2016-16352-4

Colloquia: La Thuile 2016

New Physics in final states with leptons or photons (EXO)

R. Radogna(1)(2) on behalf of the CMS Collaboration
(1) *INFN, Sezione di Bari - Bari, Italy*
(2) *Dipartimento di Fisica, Università di Bari - Bari, Italy*

received 26 July 2016

Summary. — A survey is presented of results from some recent searches for exotic physics in final states with leptons or photons such as dilepton and diphoton massive resonances or vector-like quarks searches. The results are based on 13 TeV proton-proton collisions data collected by the CMS detector at the LHC.

1. – Introduction

The Standard Model (SM) of particle physics is a successful theory supported by a wealth of experimental evidences. It is known however, that the SM does not describe the nature completely and it is usually seen as a low-energy approximation of a more general theory. There exist many theories extending beyond the SM which predict new physics at the TeV-scale that can be probed with the Large Hadron Collider (LHC) at CERN.

Due to the increase in the center-of-mass energy from 8 to 13 TeV the parton luminosities associated to new physics production processes increase very substantially in the high mass region.

We present an overview of recent results from searches for new physics in final states with leptons or photons, performed by the CMS experiment [1].

2. – Search for W′ production in the lepton+MET final state

Many SM extensions predict additional heavy gauge bosons. In particular the Sequential Standard Model (SSM) [2] predicts the existence of new massive bosons exhibiting the same couplings as the SM bosons.

A search for new physics in events with an electron or muon and missing transverse energy E_T^{miss}, which may flag the presence of a non-interacting particle (neutrino), has been performed using 2.2 fb^{-1} of pp collision data at $\sqrt{s} = 13\,\text{TeV}$, collected by the CMS detector during 2015 [3].

The main discriminant variable used in the search is the transverse invariant mass, M_T, defined from the lepton $\vec{p}_T$, the $\vec{p}_T^{miss}$ in the event, and the difference in the azimutal

angle between them, as $M_T = \sqrt{2p_T^{\ell} E_T^{miss}(1 - \cos[\Delta\phi(\vec{p}_T^{\,\ell}, \vec{p}_T^{\,miss})]}$. The quantity $\vec{p}_T^{\,miss}$ is defined as $-\Sigma\vec{p}_T$ of all reconstructed particles with E_T^{miss} being the modulus.

Events with at least one high-p_T lepton are selected requiring offline reconstructed p_T greater than 53 (130) GeV in the muon (electron) channel, where the trigger efficiency reaches the plateau. The relatively high electron threshold is required in order to suppress non-prompt electrons and jets at trigger level. Leptons and E_T^{miss} are reconstructed using a Particle-Flow technique [4, 5] and identification requirements optimized for high-p_T leptons are applied. Requirements on isolation are also included. The barrel-endcap transition region $1.444 < |\eta| < 1.566$ is excluded for the electron reconstruction, and, in the muon channel, to ensure a good muon transverse momentum determination given the preliminary detector alignment available, the pseudorapidity region $|\eta| < 2.0$ is used. In addition to high-p_T lepton cuts, the two-body decay kinematics of the $W' \to \ell\nu$ process is exploited for background suppression, and two kinematic cuts are applied: a back-to-back configuration between the lepton and $\vec{p}_T^{\,miss}$ is required ($|\Delta\phi(\vec{p}_T^{\,\ell}, \vec{p}_T^{\,miss})| > 2.5$) and the ratio of the charged lepton transverse momentum and E_T^{miss} is asked to be in the region $0.4 < p_T/E_T^{miss} < 1.5$.

The dominant and irreducible background of this search is $W \to \ell\nu$ with $\ell = \mu, e$. The tau decay channel, considered as background, contributes to the low-M_T region. Other background processes are Drell-Yan, where one of the leptons is not reconstructed, $t\bar{t}$ in their semileptonic or dileptonic decay channel, single top and dibosons. The contribution from these processes is estimated from simulation. To reduce the Drell-Yan background, events with additional muons (electrons) of $p_T > 25\,\text{GeV}$ ($E_T > 35\,\text{GeV}$) are rejected. The QCD multijet background, mostly affecting the electron channel, is largely rejected by the analysis selection criteria and the remaining contribution to the high mass region is estimated from data.

We compare the observed differential transverse mass M_T together with the predicted SM backgrounds for the electron channel (fig. 1, left) for $M_T > 200\,\text{GeV}$ and the muon channel (fig. 1, right) for values $M_T > 120\,\text{GeV}$. Simulated samples, are normalized to the integrated luminosity of the recorded dataset ($2.2\,\text{fb}^{-1}$), using calculated NNLO

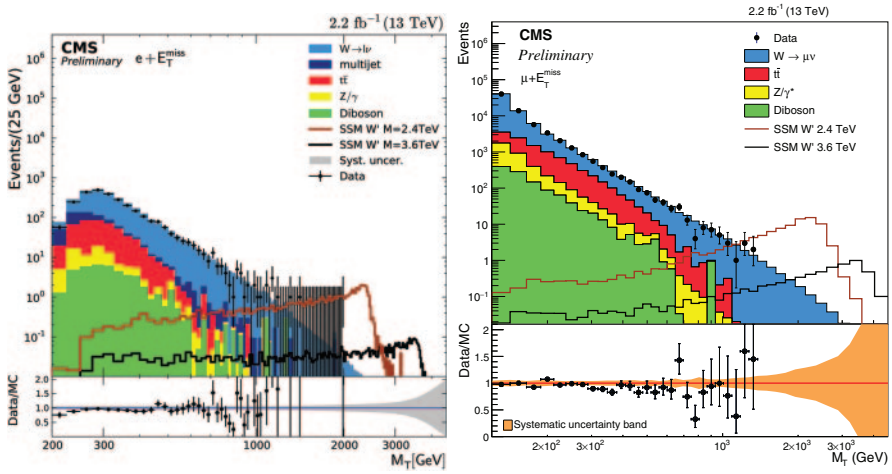

Fig. 1. – Transverse mass M_T distributions for data and expected SM backgrounds after kinematic selection in the electron (left) and muon (right) channels. The bottom panels show the ratio of observed data to SM predictions.

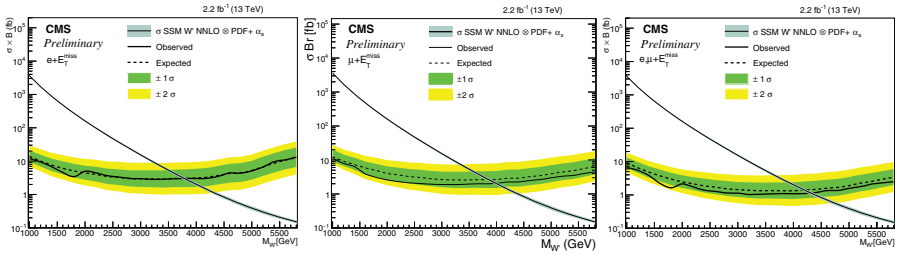

Fig. 2. – Expected and observed 95% CL limits for the electron channel (left), muon channel (middle), and the combination of both decay channels (right). The expected (observed) limit are displayed as a dashed (solid) line and the green (yellow) bands represent the ± one (two) standard deviations from this expected limit respectively. The SSM W′ NNLO cross sections are depicted as a function of $M(\mathrm{W}')$.

cross sections (NLO cross sections for the diboson samples). The bottom panels in fig. 1 show the ratio between data and SM prediction, showing good agreement between them within the given uncertainties. The expected signal from the decay of two W′ bosons with masses $M(\mathrm{W}') = 2.4$ and 3.6 TeV are also shown.

As no significant deviation from predictions is seen in the M_T distributions, we set upper limits at 95% confidence level (CL) on the production cross section times branching fraction $\sigma_{\mathrm{W}'} \times B(\mathrm{W}' \to \ell\nu)$ of a W'_{SSM} boson. No interference with the W boson from the SM is considered. The limits are provided for $M_T > 1$ TeV, where the data collected at 13 TeV are expected to be more sensitive to new physics than the dataset recorded at 8 TeV, due to the signal cross section dependence with the W′ mass for the concerned center-of-mass energies. Expected and observed limits as a function of W′ mass are shown in fig. 2 in the electron channel (left), the muon channel (middle) and the combination of both decay channels (right).

Masses below 3.8 (4.0) TeV are excluded using the individual electron (muon) decay channels analysis. When both channels are combined the limits on the mass exclusion extend to 4.4 TeV (4.2 TeV expected). These values significantly improve the results obtained with the Run-I data.

3. – Search for a Narrow Resonance in the dilepton final state

A common signature of new physics beyond the standard model is a new massive neutral spin-1 particle, referred to as a Z′, which can decay to lepton pairs. A search for such a Z′ in events with electron-positron and muon-antimuon final states has been performed using 2.8 fb^{-1} of pp collision data at $\sqrt{s} = 13$ TeV, collected by the CMS detector during 2015 [6].

The electron candidates are required to have $E_T > 35$ GeV and satisfy $|\eta| < 1.44$ (barrel region) or $1.57 < |\eta| < 2.5$ (endcap region). At least one of the electron candidates must be reconstructed in the barrel region. The electron candidates are also required to pass the HEEP (high energy electron pairs) selection [7]. Isolation criteria are also applied. Selected electron candidate pairs are not required to have opposite charge as the charge misidentification rate is large for TeV electrons.

The muon candidates are required to have $p_T > 53$ GeV and be within the sensitive region of $|\eta| < 2.4$. Requirements on isolation and specific high-p_T muon identification are also included. To ensure that the two muons originate from the same vertex a fit is performed to a common vertex, and this vertex fit is required to have $\chi^2/\mathrm{dof} < 20$.

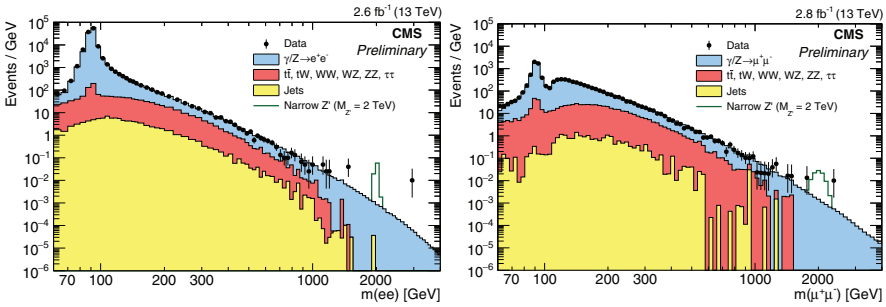

Fig. 3. – Invariant-mass distributions for data and expected SM backgrounds of dielectron (left) and dimuon (right) events.

The dominant and irreducible background of this search is $Z/\gamma^* \to \ell^+\ell^-$ with $\ell = \mu, e$. Other background are processes which produce real prompt leptons where the two prompt leptons are from different particles, usually W bosons: $t\bar{t}$, tW and dibosons processes. The contribution from these processes is estimated from simulation. The background arising from nonprompt and misidentified leptons occurs when one or more of the leptons is wrongly identified as a prompt lepton. The dominant processes in this category are dijets and W+jets events, largely rejected by the analysis selection criteria, and estimated from data. Cosmic rays hitting the detector in time with collision events are highly suppressed by requiring a reconstructed vertex in the event and applying cuts on the muons impact parameters as well as the 3D angle between the muons.

We compare the observed mass spectra together with the predicted SM backgrounds for the electron channel (fig. 3, left) and the muon channel (fig. 3, right). The Monte Carlo simulated events for all processes are normalised such that the total background prediction agrees with the data in the mass region of 60 to 120 GeV. The expected signal from the decay of two Z' bosons with masses $M(Z') = 2$ TeV is also shown. The observed mass spectrum agrees well with that of the predicted SM background.

We set upper limits at 95% CL on the ratio of the Z' cross section to the Z/γ^* cross section in a mass window of 60 to 120 GeV, assuming a narrow resonance. When calculating the limits, the electron channel is split into two channels, barrel-barrel and barrel-endcap due to differing backgrounds and resolutions.

The limits are shown in fig. 4 for signal Breit-Wigner widths of 0%, 0.6% and 3% for the electron and muon channels, both separately and combined. The latter two widths correspond to the widths of the superstring-inspired Z'_Ψ and Z'_{SSM} respectively. Figure 5 shows the observed limits for an input width of 0.6% together with the 68% and 95% expected bands. The limits exclude a Z'_{SSM} with a mass less than 3.15 TeV (3.35 TeV expected) and Z'_Ψ with a mass less than 2.60 TeV (2.80 TeV expected). This surpasses the results obtained with the Run-I data.

4. – Search for new physics in high mass diphoton events

The large difference between the scales of electroweak and gravitational interactions is known as hierarchy problem, and one of the proposals to solve it is the introduction of additional space-like dimensions in the theory in order to lowering the effective Planck scale by making the gravity acting in the additional dimensions.

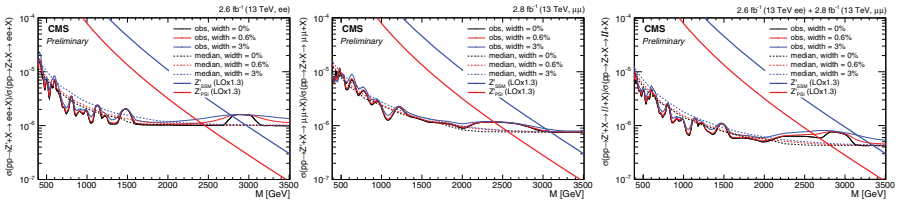

Fig. 4. – Expected and observed 95% CL limits on the cross section for Z′s of various widths for the electron channel (left), muon channel (middle) and the muon and electron channels combined (right). The expected (observed) limit are displayed as a dashed (solid) line. The cross sections do not include contributions from PDF and interference events.

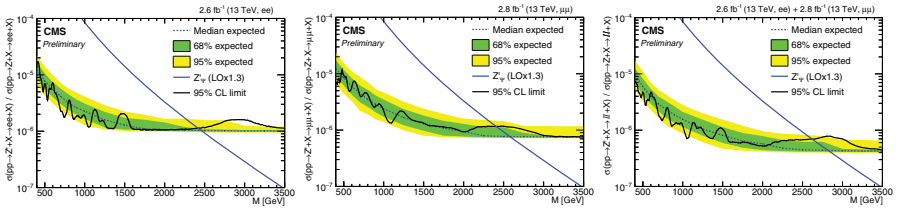

Fig. 5. – Expected and observed 95% CL limits on the on-shell cross section for a narrow Z′ modelled by a Breit-Wigner function with width 0.6% for the electron channel (left), muon channel (middle) and the muon and electron channels combined (right). The expected (observed) limit are displayed as a dashed (solid) line and the green (yellow) bands represent the ± one (two) standard deviations from this expected limit, respectively.

The Randall and Sundrum (RS) model [8] postulates the presence of two brane-worlds letting the SM fields propagate in only one of the two. The further assumption of a warped space-time metric allows the difference between the electroweak and Planck scales to be accounted for. From the phenomenological point of view, it predicts the existence of spin-2 resonances, commonly denoted as gravitons. The model is parametrised in terms of an effective coupling constant $\tilde{k} = \sqrt{8\pi}k/m_{Pl}$, where k is the curvature scale of the extra dimensions and $m_{Pl} \sim 10^{19}$ GeV is the Planck mass. The relative width of the lowest graviton resonance is $\sim 1.4\tilde{k}^2$ [9].

A search for the effect of extradimensional models in diphoton final states has been performed using $2.6\,\mathrm{fb}^{-1}$ of pp collision data at $\sqrt{s} = 13\,\mathrm{TeV}$, collected by the CMS detector during 2015 [10]. The range $0.01 < \tilde{k} < 0.2$ and resonance masses (m_G) between 500 GeV and 4.5 TeV are considered.

The photon candidates are required to have $p_T > 75\,\mathrm{GeV}$ and satisfy $|\eta| < 1.44$ (barrel region) or $1.57 < |\eta| < 2.5$ (endcap region). At least one of the photon candidates must be in the barrel region. The invariant mass of the pair, $m_{\gamma\gamma}$, is required to be above 230 GeV if both photons are in the barrel (EBEB category), above 320 GeV if one of the photon candidates is in the endcap region (EBEE category). High-p_T specific identification criteria are applied.

The dominant and irreducible background of this search is the direct production of two photons. Other backgrounds are processes which produce γ + jets and multi-jet final states. The event selection efficiencies and the background composition were measured in data and compared with expectations. Energy scale and resolution corrections are derived primarily from $Z \to e^+e^-$ events.

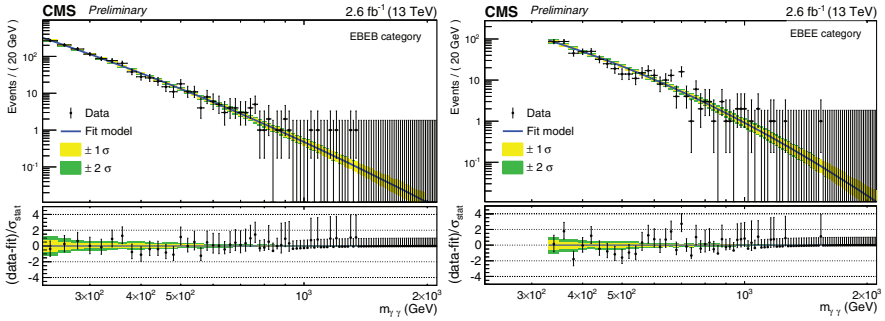

Fig. 6. – Observed invariant-mass spectrum for the EBEB (left) and EBEE (right) categories. The results of parametric fits to the data are also shown.

The observed invariant-mass distribution of the selected events is shown in fig. 6. A parametrisation of the spectrum, obtained through a maximum-likelihood fit to the selected events, is shown. This parametric form corresponds to the one chosen to model the background in the hypothesis tests. The accuracy of the background determination is assessed using MC simulations. The observed mass distribution is consistent with the expectations from the SM.

We set expected and observed upper limits at 95% CL on the production cross section times branching fraction $\sigma_G \times B_{\gamma\gamma}$ for values $\tilde{k}$ of 0.01, 0.1 and 0.2, as shown in fig. 7. A simultaneous fit to the invariant mass spectra of the the EBEB and EBEE event categories is used to study the compatibility of the data with the background-only and the signal+background hypotheses.

The limits exclude a RS graviton of mass less than 1.3, 3.1, and 3.8 TeV (1.35, 3.1 and 3.8 TeV expected) for $\tilde{k}$ of 0.01 0.1 and 0.2 respectively. These limits exceed those obtained with the Run-I data.

The compatibility of the observation with the background-only hypothesis is evaluated computing the background only p-value. The largest excess observed in data has a local significance corresponding to 2.6 standard deviations, it is observed for $m_G = 760\,\text{GeV}$ and $\tilde{k} = 0.01$ and is determined by an excess of events in the EBEB category. The global significance of this excess is estimated to be smaller than 1.2 standard deviations.

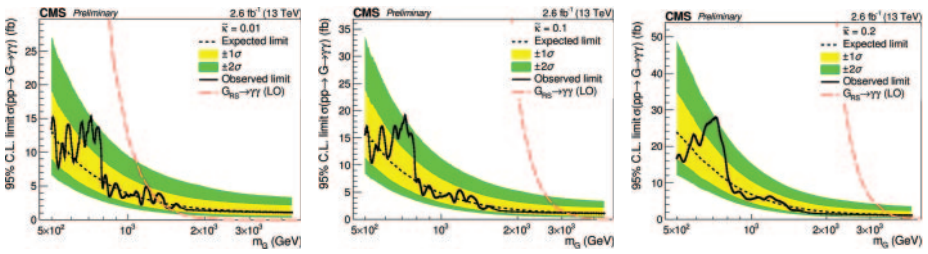

Fig. 7. – Expected and observed 95% CL limits on the cross section for RS gravitons of various widths. The range $500\,\text{GeV} < m_G < 4.5\,\text{TeV}$ is shown for $\tilde{k} = 0.01$, 0.1, 0.2 on the left, middle, right, respectively. The expected (observed) limit are displayed as a dashed (solid) line and the green (yellow) bands represent the ± one (two) standard deviations from this expected limit.

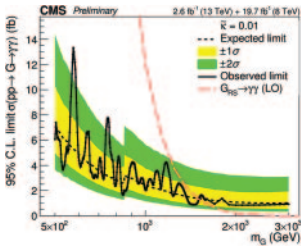

Fig. 8. – Expected and observed 95% CL limits on the cross section for RS gravitons with the combined analysis. For $m_G < 850\,\text{GeV}$, the results obtained at $\sqrt{s} = 8\,\text{TeV}$ with the analysis described in ref. [11] are combined with those obtained at 13 TeV. For $m_G > 850\,\text{GeV}$ the results of the analysis described in [12] at 8 TeV is considered for the final combination.

4˙1. *Combined analysis at* $\sqrt{s} = 8$ *TeV and 13 TeV.* – Two analyses, in the mass range between 150 and 850 GeV [11] and above 500 GeV [12], were performed by the CMS collaboration to search for RS graviton resonances decaying to two photons using the 8 TeV dataset. The statistical combination of the 13 TeV and 8 TeV results is performed taking the signal hypotheses where $\tilde{k} = 0.01$. The ratio of the signal production cross sections at 8 TeV and 13 TeV has been calculated using PYTHIA. Since the event samples selected by the two 8 TeV analyses partially overlap, only one of the two is considered at each m_G hypothesis. In particular, at each m_G, the analysis leading to the most stringent median expected exclusion limit on RS graviton production is taken. In the combined analysis, a simultaneous fit to the $m_{\gamma\gamma}$ spectra in all the event categories is performed, assuming a common signal strength for all categories.

The expected and observed upper limits at 95% CL on the production cross section times branching fraction $\sigma_G \times B_{\gamma\gamma}$ for the combined analysis are shown in fig. 8. For the signal hypotheses below roughly 1.5 TeV, the exclusion limits obtained with the combined analysis improves those obtained with the single analyses by 20–30%.

The largest excess is observed for $m_G = 750\,\text{GeV}$ and has a local significance of roughly 3 standard deviations. The global significance of the excess is estimated to be less than 1.7 standard deviations.

5. – Conclusion

In conclusion, we have presented several recent results for BSM searches by the CMS experiment, covering final states with leptons and photons and many benchmark models of BSM scenarios. Although no sign of new physics beyond the SM have been found, the Run-2 analyses have allowed to significantly improve the results obtained with the Run-I data. The search for new physics is still ongoing at the LHC and new answers will come from the analysis of 2016 13 TeV collisions.

REFERENCES

[1] CMS Collaboration, *JINST*, **3** (2008) S08004, doi:10.1088/1748-0221/3/08/S08004.
[2] Altarelli G., Mele B. and Ruiz-Altaba M., *Z. Phys. C*, **45** (1989) 109, doi:10.1007/BF01556677.
[3] CMS Collaboration, CMS PAS EXO-15-005 (2015).

[4] CMS Collaboration, *Particle-flow event reconstruction in CMS and performance for jets, taus, and* E_T^{miss}, CMS-PAS-PFT-09-001 (2009).
[5] CMS Collaboration, *Commissioning of the particle-flow event reconstruction with the first LHC collisions recorded in the CMS detector*, CMS-PAS-PFT-10-011 (2010).
[6] CMS Collaboration, CMS PAS EXO-15-006 (2015).
[7] CMS Collaboration, *JINST*, **10** (2015) P06005, doi:10.1088/1748-0221/10/06/P06005.
[8] Randall L. and Sundrum R., *Phys. Rev. Lett.*, **83** (1999) 3370, doi:10.1103/PhysRevLett.83.3370.
[9] Davoudiasl H., Hewett J. L. and Rizzo T. G., *Phys. Rev. Lett.*, **84** (2000) 2080, doi:10.1103/PhysRevLett.84.2080.
[10] CMS Collaboration, CMS PAS EXO-15-004 (2015).
[11] CMS Collaboration, *Phys. Lett. B*, **750** (2015) 494, doi:10.1016/j.physletb.2015.09.062.
[12] CMS Collaboration, *Search for High-Mass Diphoton Resonances in pp Collisions at* $\sqrt{s} = 8$ *TeV with the CMS Detector*, CMS-PAS-EXO-12-045 (2012).